Supporting Information

Ramaglia et al. 10.1073/pnas.1111924109

SI Results

Alternative Pathway Activation in Complement Receptor 1-Related Protein y (Crry)$^{-/-}$ Spinal Cord. C3 mRNA expression by quantitative PCR (qPCR) was increased more than twofold in Crry$^{-/-}$ and factor H (fH)$^{-/-}$ spinal cords compared with WT ($P < 0.05$ for each comparison, one-way ANOVA) (Fig. 2*G*), confirming that C3 synthesis is up-regulated to a similar degree in both Crry$^{-/-}$ and fH$^{-/-}$ mice.

Lack of the Crry$^{-/-}$ microglial-primed phenotype in Crry$^{-/-}$fB$^{-/-}$ mice (Fig. 1*D*) suggested involvement of the alternative pathway. To determine whether other alternative pathway components were up-regulated, mRNA levels of fB and fD as well as alternative pathway regulators decay-accelerating factor (DAF), fH, and Crry were measured by qPCR in spinal cords of WT, Crry$^{-/-}$, and fH$^{-/-}$ mice. Expression of fB (Fig. 2*H*) and fD (Fig. 2*I*) mRNAs was increased by ∼50% in both Crry$^{-/-}$ and fH$^{-/-}$ spinal cords compared with WT (each comparison, $P < 0.05$, one-way ANOVA), confirming that all components of the alternative pathway amplification loop were up-regulated; no significant changes in mRNA levels of the complement regulators DAF (Fig. 2*J*), fH (Crry$^{-/-}$ only; Fig. 2*K*), and Crry (fH$^{-/-}$ only; Fig. 2*L*) were observed in either knockout strain.

Soluble Complement Receptor 1 (sCR1) Treatment Inhibits LPS-Induced CNS Inflammation in Crry$^{-/-}$ Mice. Mice were injected i.p. with sCR1 at 12 h before LPS challenge. sCR1 has a half-life of 24 h in rodents and crosses the blood–brain barrier (BBB) in the context of inflammation (1, 2). Systemic C3 consumption was inhibited in Crry$^{-/-}$ mice as shown by a 2.7-fold increase in intact C3 in plasma at 12 h, returning C3 to WT levels (Fig. 3 *K* and *L*). Treatment with sCR1 significantly reduced LPS up-regulation of all five inflammatory markers in spinal cord (Fig. 3 *A–D* and *F*) and hippocampus (Fig. S4 *A–D* and *F*), reduced LPS-triggered increase in IL-1β immunoreactivity in spinal cord (Fig. 3*J*), and ameliorated LPS-induced lethargy.

SI Materials and Methods

Animal Genotyping and Housing. Crry deficiency was confirmed by PCR with specific primers (3). Genotyping of Crry$^{-/-}$C3$^{-/-}$, Crry$^{-/-}$fB$^{-/-}$, and fH$^{-/-}$ mice was performed as described (4). Throughout the paper, mice solely deficient in Crry are sometimes referred to as C-sufficient Crry$^{-/-}$ to discriminate them from mice that are also genetically deficient in C3 or fB. WT C57BL/6 mice maintained under identical conditions were used as controls in all studies. Mice were screened for microbiological status, housed under standard pathogen-free conditions, and allowed free access to food and water. Male mice aged 10 or 32 wk were used in all experiments. All experiments complied with national guidelines for animal care.

Western Blot Analysis. Complement activation was assessed in fresh plasma from treated and untreated WT and Crry$^{-/-}$ mice by separation of plasma (1 μL) on 7.5% SDS/PAGE and Western blotting with rabbit anti-mouse C3 (0.4 μg/mL; Hycult) to detect C3 fragments as previously described (3). Intact C3 α-chain was quantified by densitometry using Image Pro Plus 6.00 software (Media Cybernetics) on three independent blots. Values are expressed as mean ± SD of the integrated optical density (IOD) for the immunoreactive band per group of mice. The experiment was performed in triplicates.

Immunohistochemistry. Staining was developed by using either 3,3-diaminobenzidine tetrahydrochloride (DAB; Vector Laboratories) or 3-amino-9-ethylcarbazole (AEC; Sigma-Aldrich) and counterstained with hematoxylin. Sections stained with isotype control or primary or secondary conjugate alone were included as negative controls. After dehydration, slides were mounted in Pertex (Histolab).

Slides were mounted in anti-fade medium (FluorSave Reagent; Calbiochem). Images were captured digitally from a fluorescence microscope (DM LB2; Leica) and analyzed with Image Pro Plus 6 software (Media Cybernetics).

In Situ Hybridization. In situ hybridization for DAF was performed with a 5′ fluorescein-labeled 19-mer antisense oligonucleotide containing locked nucleic acid and 2′ *O*-methyl RNA moieties (mouse probe sequence: FAM, TuuGucAcaTgaAuaGguG; human probe sequence: FAM, TauGccAccTggTacAucA; uppercase indicates LNA, and lowercase indicates 2′ *O*-methyl RNA) as previously described (5).

Treatment of Experimental Autoimmune Encephalomyelitis (EAE) Crry$^{-/-}$ Mice with sCR1. An additional group of seven Crry$^{-/-}$ mice aged 10 wk were subject to the EAE immunization protocol as previously described (6). As an additional control, four Crry$^{-/-}$ mice were treated with PBS and three Crry$^{-/-}$ mice were treated with sCR1 (15 mg/kg i.p.) daily from day 8 post-immunization. These mice were killed on day 14 before they developed significant clinical signs. In all cases, spinal cords were harvested; quartered approximating to cervical, thoracic, lumbar, and sacral regions; and processed for histology.

Treatment of Naïve Crry$^{-/-}$ Mice with sCR1. Four Crry$^{-/-}$ mice were treated systemically with sCR1 (15 mg/kg i.p.) daily for 1 wk. Brains and spinal cords were collected and processed in formalin for histology.

Quantitative Analysis of Immunohistochemistry. For all quantitative analysis of the immunohistochemical staining, at least four nonconsecutive sections were scored for each animal in each group. Staining for hematoxylin, ionized calcium-binding adaptor molecule 1 (Iba-1), IL-1β, and Luxol fast blue (LFB) are expressed as percentage stained of total area examined. For CD11b, immunoreactive cells associated with nuclear hematoxylin staining were counted on six to eight nonoverlapping fields, including >90% of the white matter (wm) or gray matter (gm), and expressed as number of cells per mm^2. CD11b-positive cytoplasmic protrusions of a cell not associated to a nucleus were not counted. For comparative analyses, equivalent perivascular areas from WT and Crry$^{-/-}$ mice were scored. All values are expressed as mean ± SD per group of mice.

Multiple Sclerosis (MS) Tissue Analyses. Archival, formalin-fixed, paraffin-embedded brain tissue, collected with written informed consent and full clinical information, was obtained from the Netherlands Brain Bank (Netherlands Institute for Neuroscience, Amsterdam). Nine MS cases and four matched nonneurological controls (Table S1) were analyzed. Cases were selected to provide a spectrum of activity from chronic active to gliotic inactive lesions. Sections (6 μm) were stained with H&E, LFB for myelin, and Palmgren's silver stain for axons to identify the plaque core (LFB-negative, reduced H&E, and Palmgren staining), rim (border between LFB-positive and LFB-negative), perilesional white matter (LFB-positive area extending 2 mm from plaque rim), and normal-appearing white matter (LFB-positive area further re-

moved from plaque). Sections were stained as described above for all three subunits (HLA-DP, HLA-DQ, and HLA-DR) of the HLA (HLA-DP-DQ-DR) (microglial marker, mAb CR3/43; Dako), IL-1β [in-house rabbit polyclonal Ab (7)], and C3b/iC3b/C3c (rabbit polyclonal Ab; Dako), referred to here as C3b/iC3b because the soluble C3c fragment is not retained in tissue. Anti-C3b/iC3b had been adsorbed against human plasma proteins to remove reactivity against native C3. Quantification of staining was performed by two independent observers (V.R. and I.H.).

Statistical Analysis. ANOVA with Bonferroni correction was performed for immunohistochemistry, qPCR analysis of cytokine expression, and densitometric analysis of Western blots. Mann–Whitney *U* nonparametric test was performed for EAE clinical score. Student's *t* test was performed for the qPCR analysis of complement components and regulators and quantitative analysis of EAE histology and immunohistochemistry (H&E, IL-1β, and LFB). Two-tailed *P* values are quoted throughout.

Characterization of CNS Changes in Crry$^{-/-}$ Mice. Groups of three WT and three Crry$^{-/-}$ mice aged 10 wk and four WT and four Crry$^{-/-}$ mice aged 32 wk were killed by transcardial perfusion with PBS followed by 10% buffered formalin. Brains and spinal cords were removed and postfixed in 4% paraformaldehyde in PBS for standard processing in paraffin wax for histology. Additional groups of three WT and three Crry$^{-/-}$ mice aged 10 wk and four WT and four Crry$^{-/-}$ mice aged 32 wk were perfused with PBS, and brains and spinal cords were harvested and divided into two portions: one embedded in O.C.T. (Sakura) for immunohistochemistry and the other directly frozen in liquid nitrogen and stored at −80 °C for mRNA analysis. Spinal cords from three Crry$^{-/-}$C3$^{-/-}$, three Crry$^{-/-}$fB$^{-/-}$, and four fH$^{-/-}$ mice aged 10 wk were also analyzed.

Peripheral LPS Challenge in Crry$^{-/-}$ Mice. Five WT and eight Crry$^{-/-}$ mice aged 10 wk were injected i.p. with LPS (*Salmonella enterica* serotype Typhimurium, 100 μg/kg in PBS, L6143; Sigma-Aldrich), a dose chosen to trigger microglial activation (8). Matched controls, three WT and four Crry$^{-/-}$ mice, were given nonpyrogenic PBS i.p. Additional matched groups of four WT and four Crry$^{-/-}$ mice were treated at 12 h before LPS challenge with sCR1 (20 mg/kg in PBS i.p.; TCS), a dose shown in previous studies to inhibit C activation in rodents (9, 10). Matched controls, three WT and three Crry$^{-/-}$ mice, received PBS before LPS challenge. In a separate experiment, groups of 15 WT and 19 Crry$^{-/-}$ mice aged 32 wk were challenged with LPS as above.

In all experiments, mice were bled and killed by PBS perfusion at 2 h after LPS challenge. Spinal cords and brains were collected and portioned for histology (postfixed in 4% paraformaldehyde), immunohistochemistry (in O.C.T. as above), or RNA analysis (snap-frozen in liquid N_2). Plasma was harvested for measurement of IL-6 and TNF-α by ELISA (Quantikine; R&D Systems).

Induction of EAE. EAE was induced in four WT and six Crry$^{-/-}$ mice aged 10 wk as previously described (11). Four Crry$^{-/-}$ mice aged 10 wk were subject to the same immunization protocol but without myelin oligodendrocyte glycoprotein (MOG) in the adjuvant mix. Mice were monitored daily for signs of disease until they reached the limit of clinical disability as previously published (11). In all cases, spinal cords were harvested; quartered approximating to cervical, thoracic, lumbar, and sacral regions; and processed as described above.

1. Piddlesden SJ, et al. (1994) Soluble recombinant complement receptor 1 inhibits inflammation and demyelination in antibody-mediated demyelinating experimental allergic encephalomyelitis. *J Immunol* 152:5477–5484.
2. Ramaglia V, et al. (2008) Soluble complement receptor 1 protects the peripheral nerve from early axon loss after injury. *Am J Pathol* 172:1043–1052.
3. Ruseva MM, et al. (2009) Crry deficiency in complement sufficient mice: C3 consumption occurs without associated renal injury. *Mol Immunol* 46:803–811.
4. Pickering MC, et al. (2002) Uncontrolled C3 activation causes membranoproliferative glomerulonephritis in mice deficient in complement factor H. *Nat Genet* 31:424–428.
5. Aronica E, et al. (2010) Expression pattern of miR-146a, an inflammation-associated microRNA, in experimental and human temporal lobe epilepsy. *Eur J Neurosci* 31: 1100–1107.
6. Griffiths MR, Neal JW, Fontaine M, Das T, Gasque P (2009) Complement factor H, a marker of self protects against experimental autoimmune encephalomyelitis. *J Immunol* 182:4368–4377.
7. Copray JC, et al. (2001) Expression of interleukin-1β in rat dorsal root ganglia. *J Neuroimmunol* 118(2):203–211.
8. Cunningham C, et al. (2009) Systemic inflammation induces acute behavioral and cognitive changes and accelerates neurodegenerative disease. *Biol Psychiatry* 65: 304–312.
9. Ramaglia V, et al. (2008) Soluble complement receptor 1 protects the peripheral nerve from early axon loss after injury. *Am J Pathol* 172:1043–1052.
10. Piddlesden SJ, et al. (1994) Soluble recombinant complement receptor 1 inhibits inflammation and demyelination in antibody-mediated demyelinating experimental allergic encephalomyelitis. *J Immunol* 152:5477–5484.
11. Griffiths MR, Neal JW, Fontaine M, Das T, Gasque P (2009) Complement factor H, a marker of self protects against experimental autoimmune encephalomyelitis. *J Immunol* 182:4368–4377.

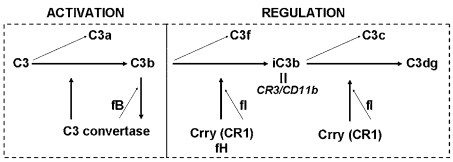

Fig. S1. Schematic representation of the alternative pathway activation and regulation of C3. The ligand for iC3b, CR3 (detected by the CD11b marker on microglia), is shown in italic. The human homolog of Crry, complement receptor 1 (CR1), is shown in parentheses.

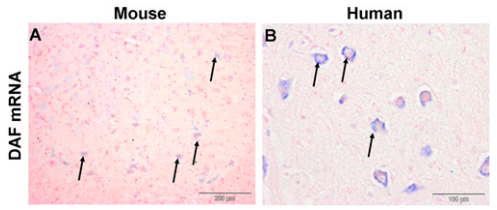

Fig. S2. DAF expression in mouse spinal cords and human brains. In situ hybridization for DAF in mouse spinal cords (*A*, $n = 7$ mice) and human brains (*B*, $n = 4$ cases) showing expression in neurons, whereas glial cells are virtually negative. Arrows indicate stained neurons in both *A* and *B*. Note scale bar in *A* is 200 μm, whereas scale bar in *B* is 100 μm to visualize mouse and human neurons, respectively. Antibody isotype controls and mismatch oligonucleotide controls were always negative.

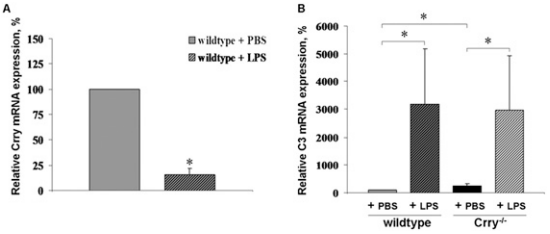

Fig. S3. Spinal cord expression of Crry and C3 after systemic LPS challenge. (*A*) Relative Crry mRNA expression in spinal cords of WT mice before ($n = 3$) and at 2 h after ($n = 5$) systemic LPS challenge. (*B*) Relative C3 mRNA expression in spinal cords of WT and Crry$^{-/-}$ mice before (WT $n = 3$; Crry$^{-/-}$ $n = 4$) and at 2 h after (WT $n = 5$; Crry$^{-/-}$ $n = 8$) systemic LPS challenge. Values are normalized to the expression of β-actin and given as percentage (means ± SD) of WT control levels. Error bars are for *n*, number of animals. *$P < 0.001$ in *A*, determined by two-tailed Student's *t* test; *$P \leq 0.001$ in *B*, determined by one-way ANOVA.

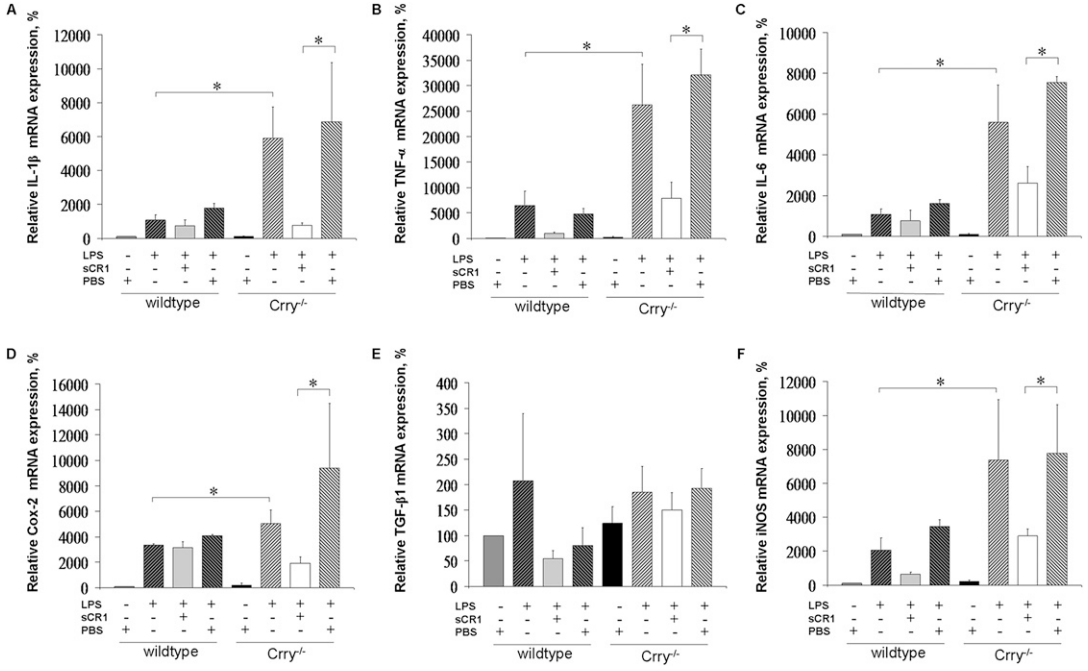

Fig. S4. Hippocampal expression of inflammatory mediators is up-regulated in Crry$^{-/-}$ mice after systemic LPS challenge. Relative mRNA expression of IL-1β (*A*), TNF-α (*B*), IL-6 (*C*), Cox-2 (*D*), TGF-β1 (*E*), and inducible nitric oxide synthase (iNOS) (*F*) in hippocampi of WT and Crry$^{-/-}$ mice before (–LPS; WT $n = 3$; Crry$^{-/-}$ $n = 4$) and after (+LPS; WT $n = 5$; Crry$^{-/-}$ $n = 8$) systemic challenge with LPS, either with (+sCR1; WT $n = 4$; Crry$^{-/-}$ $n = 4$) or without (+PBS; WT $n = 3$; Crry$^{-/-}$ $n = 3$) pretreatment with sCR1. Values are normalized to the expression of β-actin and given as percentage (means ± SD) of WT control levels. Error bars are for *n*, number of animals. Asterisks indicate statistically significant differences determined by one-way ANOVA. Specific *P* values for each gene are given in the text.

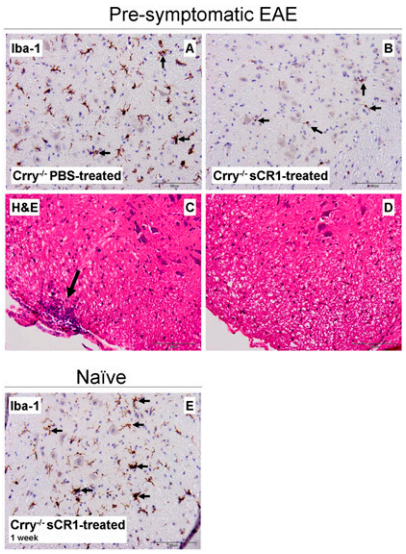

Fig. S5. (*A* and *B*) Immunostaining for the Iba-1 marker of macrophages in spinal cords of Crry$^{-/-}$ mice at day 14 in the course of induction of EAE treated with either PBS (n = 4) from day 8 and showing primed microglial morphology (*A*, arrows) or sCR1 (n = 4) from day 8 and showing quiescent microglial morphology (*B*, arrows). (*C* and *D*) H&E staining of spinal cords from EAE Crry$^{-/-}$ mice treated with either PBS or sCR1 as above, showing meningeal, subpial, and perivascular accumulation of inflammatory cells in the spinal cords of Crry$^{-/-}$ PBS-treated mice (*C*), whereas no inflammatory infiltrates were present in spinal cords of Crry$^{-/-}$ sCR1-treated mice (*D*). (*E*) Immunostaining for Iba-1 in spinal cords of Crry$^{-/-}$ mice treated with sCR1 for 1 wk (n = 4) and showing primed microglial morphology (arrows).

Table S1. Clinical and neuropathological data of cases

Subject no.	Sex	Age, y	PMD, h:min	Disease duration, y	MS type	Cause of death
MS						
1	F	41	08:25	11	SP	Natural death
2	M	51	07:50	29	ND	Uremia/cachexia
3	M	43	08:30	17	SP	Pneumonia
4	M	53	05:30	3	PP	Respiratory insufficiency
5	F	48	08:10	9	ND	Euthanasia
6	F	48	04:50	25	SP	Euthanasia
7	M	65	10:35	25	PP	Urosepsis
8	M	59	22:15	32	PP	Cardiac arrest
9	M	63	07:05	25	PP	Cardiac arrest
Nondemented controls						
10	F	49	09:50	–	–	Sudden death
11	M	51	07:44	–	–	Heart failure
12	M	56	14:00	–	–	Heart failure
13	M	56	09:15	–	–	Heart failure

MS type, type of MS at time of death; ND, not determined; PMD, postmortem delay until end of autopsy; PP, primary progressive; SP, secondary progressive.

Table S2. Semiquantification of HLA-DP-DQ-DR, IL-1β, and C3b/iC3b immunoreactivity in normal-appearing white matter of MS brains

Subject no.	HLA-DP-DQ-DR	IL-1β	C3b/iC3b
MS			
1	++	–	+++
2	++	–	++
3	++	–	+++
4	++	–	+++
5	++	–	+
6	++	– (bv +)	+
7	++	–	+
8	++	–	+
9	++	–	+
Nondemented controls			
10	–	–	–
11	–	–	–
12	–	–	–
13	–	–	–

–, Negative; +/–, sporadic immunoreactivity; +, low immunoreactivity; ++, high immunoreactivity; bv, blood vessel.

Table S3. TaqMan primer sequences

Target gene	Accession no.	Primer	Sequence (5′ → 3′)
Mouse complement components and regulators			
C3	NM_009778	Forward	AAGCATCAACACACCCAACA
		Reverse	CTTGAGCTCCATTCGTGACA
fB	NM_008198	Forward	ACCGCAGGACTTTGAAAATG
		Reverse	TCCAGCTCCATCATCACAAA
fD	NM_013459	Forward	CAAGCGATGGTATGATGTGC
		Reverse	CCGGGTTCCACTTCTTTGT
fH	NM_009888	Forward	GCACCCAGGCTACCTACAAA
		Reverse	AGATCCAACTGCCAGCCTAA
Crry	NM_013499	Forward	CCCATCACAGCTTCCTTCTG
		Reverse	CTTCAGCACTCGTCCAGGTT
CD55	NM_010016	Forward	CTTGCCTTGAGGATTTAGTATGG
		Reverse	CTAGCCTGTACCCTGGGTTG
Cytokines			
IL-1β	NM_008361	Forward	GCACACCCACCCTGCA
		Reverse	ACCGCTTTTCCATCTTCTTCTT
Cox-2	NM_011198	Forward	CCACTTCAAGGGAGTCTGGA
		Reverse	GAGAAGGCTTCCCAGCTTTT
IL-6	NM_031168	Forward	TCCAGAAACCGCTATGAAGTTC
		Reverse	CACCAGCATCAGTCCCAAGA
TNF-α	NM_013693	Forward	CTCCAGGCGGTGCCTATG
		Reverse	GGGCCATAGAACTGATGAGAGG
iNOS	NM_010927	Forward	TTCCAGAATCCCTGGACAAG
		Reverse	GGTCAAACTCTTGGGGTTCA
TGF-β1	NM_011577	Forward	CGTGGAAATCAACGGGATCA
		Reverse	GGCCATGAGGAGCAGGAA

Table S4. Antibodies for immunohistochemistry

Antibody	Clone	Source	Concentration/dilution
Primary			
Monoclonal rat anti-mouse C3b/iC3b/C3c (active fragments but not native C3)	3/26	Gift from Anna Erdei (Eötvös Loránd University, Budapest)	200 μg/mL
Monoclonal rat anti-mouse CD11b (unconjugated or Alexa Fluor 488-conjugated)	M1/70	BD Pharmingen	1:100
Monoclonal mouse anti-human HLA-DP-DQ-DR	CR3/43	Dako	1:100
Polyclonal rabbit anti-mouse Iba-1		Wako	1:500
Polyclonal rabbit anti-human IL-1β		Made in-house	1:500
Polyclonal rabbit anti-human C3b/iC3b/C3c (C3 active fragments)		Dako	4 μg/mL
Polyclonal goat anti-mouse Cox-2		Santa Cruz Biotechnology	2 μg/mL
Polyclonal goat anti-mouse IL-1β		R&D Systems	15 μg/mL
Secondary (biotinylated)			
Polyclonal goat anti-rat		Vector Laboratories	7.5 μg/mL
Polyclonal goat anti-mouse		Vector Laboratories	7.5 μg/mL
Polyclonal goat anti-rabbit		Vector Laboratories	7.5 μg/mL
Polyclonal rabbit anti-goat		Vector Laboratories	7.5 μg/mL